

Synthesis of single-component metallic glasses by thermal spray of nanodroplets on amorphous substrates

Qi An, Sheng-Nian Luo, William A. Goddard, W. Z. Han, B. Arman et al.

Citation: *Appl. Phys. Lett.* **100**, 041909 (2012); doi: 10.1063/1.3675909

View online: <http://dx.doi.org/10.1063/1.3675909>

View Table of Contents: <http://apl.aip.org/resource/1/APPLAB/v100/i4>

Published by the [American Institute of Physics](http://www.aip.org).

Related Articles

Mechanism of densification in silica glass under pressure as revealed by a bottom-up pairwise effective interaction model

J. Chem. Phys. **136**, 134508 (2012)

Design of ductile bulk metallic glasses by adding “soft” atoms

Appl. Phys. Lett. **100**, 141901 (2012)

Energy transfer and energy level decay processes in Tm³⁺-doped tellurite glass

J. Appl. Phys. **111**, 063105 (2012)

Molecular packing in highly stable glasses of vapor-deposited tris-naphthylbenzene isomers

J. Chem. Phys. **136**, 094505 (2012)

Continuous-annealing method for producing a flexible, curved, soft magnetic amorphous alloy ribbon

J. Appl. Phys. **111**, 07A309 (2012)

Additional information on *Appl. Phys. Lett.*

Journal Homepage: <http://apl.aip.org/>

Journal Information: http://apl.aip.org/about/about_the_journal

Top downloads: http://apl.aip.org/features/most_downloaded

Information for Authors: <http://apl.aip.org/authors>

ADVERTISEMENT

More Than 150
USB DAQ Modules

With Windows 7
and LabVIEW Support



DATA TRANSLATION®
www.datatranslation.com

Synthesis of single-component metallic glasses by thermal spray of nanodroplets on amorphous substrates

Qi An,¹ Sheng-Nian Luo,^{2,a)} William A. Goddard III,^{1,b)} W. Z. Han,² B. Arman,² and William L. Johnson³

¹Materials and Process Simulation Center, California Institute of Technology, Pasadena, California 91125, USA

²Los Alamos National Laboratory, Los Alamos, New Mexico 87545, USA

³Keck Engineering Laboratories, California Institute of Technology, Pasadena, California 91125, USA

(Received 6 September 2011; accepted 6 December 2011; published online 26 January 2012)

We show that single component metallic glasses can be synthesized by thermal spray coating of nanodroplets onto an amorphous substrate. We demonstrate this using molecular dynamics simulations of nanodroplets up to 30 nm that the spreading of the nanodroplets during impact on a substrate leads to sufficiently rapid cooling (10^{12} – 10^{13} K/s) sustained by the large temperature gradients between the thinned nanodroplets and the bulk substrate. However, even under these conditions, in order to ensure that the glass transition outruns crystal nucleation, it is essential that the substrate be amorphous (eliminating sites for heterogeneous nucleation of crystallization). © 2012 American Institute of Physics. [doi:10.1063/1.3675909]

Bulk metallic glasses (BMGs) provide a number of unique properties (ductility, high strength, high corrosion resistance, and soft magnetism), but most metallic glasses have required very high quenching rates,^{1–8} leading only to thin films of amorphous material. A great deal of progress has been made toward synthesizing bulk amorphous metallic glasses since the original successes in 1960 using cooling rates of 10^6 K/s.^{1–5} Indeed with multicomponent metals having dramatically different character and radii, it is possible to obtain amorphous sheets of cm size for numerous applications.^{1–5} Here, we take up the **challenge of forming single-component metallic glasses** (SCMGs), which might have unique surface and bulk properties. Because of the low glass-forming ability of pure metals, it has not been possible previously to make SCMG without extremely high quenching rates.

We propose here that SCMGs can be achieved by thermal spray coating of nanodroplets onto an amorphous substrate (ND-AS). We show that nanodrops of diameter ≤ 30 nm lead to sufficiently high cooling rates due to the rapid spreading of the nanodroplet during impact on the substrate, which leads to rapid cooling sustained by the large temperature gradients between the thinned nanodroplets and the bulk substrate. However, even under these conditions, we show that for glass formation to outrun crystal nucleation it is required that the substrate be amorphous (avoiding the heterogeneous nucleation sites that could lead to crystallization).

To demonstrate thermal spray ND-AS formation of SCMG, we performed molecular dynamics (MD) simulations of nanodrops of Cu up to 30 nm (1 million atoms) sprayed onto a Cu-Zr amorphous substrate ($\text{Cu}_{46}\text{Zr}_{54}$) system using force fields (potentials) validated to provide an accurate description of these metals. Our MD simulations show that these Cu SCMGs are thermodynamically stable for the

simulation time scales (up to 3 ns). In contrast, spraying the same Cu nanodroplets onto Cu crystal substrates leads to crystallization within 100 ps.

Our MD simulations used the embedded-atom-method potential for the Cu-Zr system⁹ and the LAMMPS MD package (large-scale atomic/molecular massively parallel simulator).¹⁰ We constructed liquid Cu droplets with diameters of 10 nm (39 081 atoms), which we equilibrated at 1300 K using constant-volume-temperature MD (no periodic boundary conditions). These nanodroplets were impacted on two different substrates at 300 K and 1 atm: (a) $\text{Cu}_{46}\text{Zr}_{54}$ glass; (b) Cu (100) single crystal.

For the prototypical amorphous alloy substrate, we started with randomly positioned Cu and Zr atoms for the $\text{Cu}_{46}\text{Zr}_{54}$ composition, melted at 2000 K for 0.5 ns, and then cooled continuously to 300 K within 2 ns to form the bulk glass. Then, to form the $\text{Cu}_{46}\text{Zr}_{54}$ glass substrate, we constructed from the bulk system a slab containing 320 000 atoms ($4.85 \text{ nm} \times 34.21 \text{ nm} \times 35.91 \text{ nm}$ along the x -, y - and z -axes, respectively, with the yz plane as the surface), which we annealed at 1000 K for 4 ns and then cooled to 300 K using constant-pressure-temperature (NPT) MD to form the amorphous substrate.

As a prototypical crystalline substrate, we used Cu (100) containing 432 000 atoms ($10.96 \text{ nm} \times 21.93 \text{ nm} \times 21.93 \text{ nm}$). Here, we started with the bulk FCC structure, formed the 10.96 nm thick (x direction) slab, and equilibrated at 300 K and 1 atm using NPT MD.

The Cu nanodroplet was assigned an initial impact velocity along the x -axis (the substrate normal) and impacted the substrate. The impact velocity was varied from 0.01 km/s to 0.5 km/s. We used the microcanonical ensemble for impact simulations. The time step in MD simulation was 1 fs, and the total simulation time was up to ~ 3 ns.

Fig. 1 shows the radial distribution functions (RDF) of Cu nanodroplets after impacting on crystalline and amorphous substrates. The resulting structures of the solidified

^{a)}Electronic mail: sluo@lanl.gov.

^{b)}Electronic mail: wag@wag.caltech.edu.

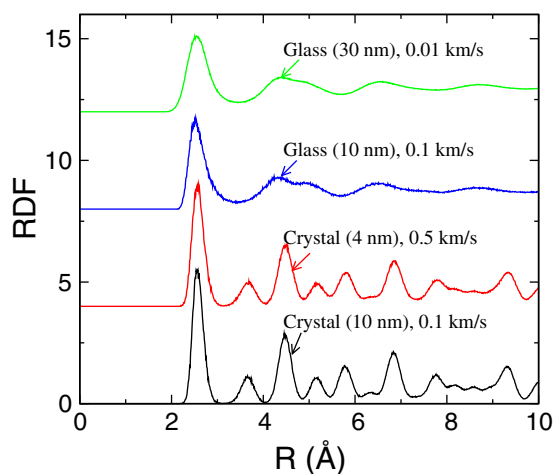


FIG. 1. (Color online) Radial distribution functions of various nanodroplets after impacting on various substrates at various impact velocities. The Cu nanodroplets form nanocrystals on the Cu crystal substrate but become amorphous glasses on the $\text{Cu}_{46}\text{Zr}_{54}$ glass substrate.

nanoparticles in the crystal substrate cases show the long-range order characteristic of crystals. On the other hand, the loss of the long-range order in the glass substrate cases indicates that the “solidified” nanoparticles are still amorphous.

The RDF only reveals the average structure information. To characterize the local structure of the amorphous Cu nanoparticle formed on the $\text{Cu}_{46}\text{Zr}_{54}$ glass substrate, we performed the Honeycutt-Anderson (HA) analysis^{11–14} on various nanoparticles at equilibrium after impact. Fig. 2 shows the equilibrium configurations and the HA structure analysis of the Cu nanoparticles after impact. On the crystalline substrate, a Cu nanocrystal grows epitaxially with growth twins and stacking faults (Figs. 2(a) and 2(b)). The characteristic HA indices of this nanocrystal are mainly 1421, corresponding to the FCC structure (Fig. 2(e)).

In sharp contrast, the impact with the $\text{Cu}_{46}\text{Zr}_{54}$ glass substrate leads to an amorphous Cu nanoparticle (Figs. 2(c) and 2(d)). HA indices 1551 and 2331 are the main characteristics of icosahedral packing, and are similar for $\text{Cu}_{46}\text{Zr}_{54}$ glass, Cu glass and Cu liquid; this indicates that the amorphous Cu nanoparticle is similar in short-to-medium-range atomic packing to the $\text{Cu}_{46}\text{Zr}_{54}$ glass and to Cu liquid (Fig. 2(e)).

To verify that the amorphous nanoparticle is indeed “solidified” as a glass (rather than remaining a liquid), we calculated the mean square displacement (MSD) of the Cu nanodroplet after the system reaches equilibrium, from which we extracted the diffusion coefficient (D) using the Einstein relation ($\text{MSD} = 6D \times \text{time}$). At 300 K, $D = 3.6 \times 10^{-5} \text{ cm}^2/\text{s}$ for the liquid nanodroplet, which is 50 times higher than $D = 8.0 \times 10^{-7} \text{ cm}^2/\text{s}$ for the amorphous nanoparticle. Thus, the amorphous nanoparticle is a solid-like SCMG.

To identify the point at which a phase transition occurs, it is valuable to determine the change in entropy with time and temperature. To extract the entropy evolution of the nanodroplets during the dynamic impact process, we used the Lin-Blanco-Goddard two phase thermodynamic (2PT) model¹⁵ to obtain the entropy of the nanodroplets impacting on the substrates. 2PT has been applied to various systems^{15–18} to obtain accurate entropies.

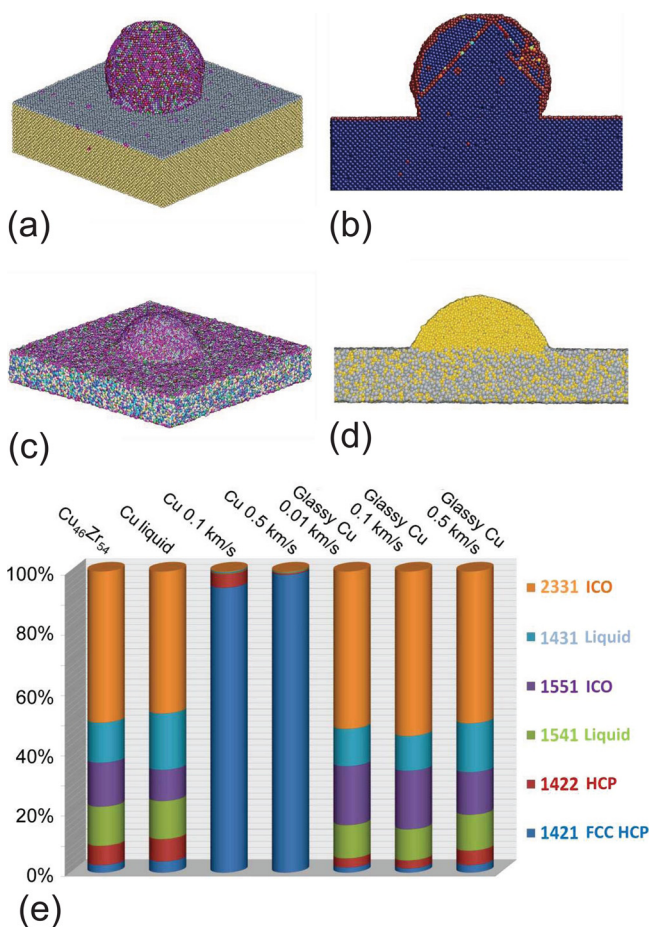


FIG. 2. (Color online) Snapshots of Cu nanodroplet (10 nm in diameter) impacting at 0.1 km/s on (a, b) a Cu single crystal substrate and (c, d) on a $\text{Cu}_{46}\text{Zr}_{54}$ glass substrate. (e) analyzes the structure of crystalline, liquid, and glassy Cu and $\text{Cu}_{46}\text{Zr}_{54}$ glass using the Honeycutt-Anderson (HA) metric. Here, 1421 is characteristic of FCC (face-centered cubic) structure while equal amounts of 1421 and 1422 are characteristic of HCP (hexagonal close-packed) structure. On the other hand, 2331 and 1551 indicate icosahedral packing characteristic of liquid or glassy metals; also 1431 and 1541 indices show the structure of liquid state.^{11–14} (b) and (d) are cross-sectional views; here, (b) shows some growth twins and FCC stacking faults. The HA indices for $\text{Cu}_{46}\text{Zr}_{54}$ glass, Cu glasses, and Cu liquids all contain the icosahedral HA indices (2331 and 1551) of a liquid or glass but drastically different from those for crystalline Cu (e.g., 1421).

We examined nanodroplets of 4 nm in diameter with impact velocity of 0.5 km/s and applied the 2PT model along the impact trajectory (up to 90 ps). The average temperature and entropy were extracted every 2 ps from 2PT model as shown in Fig. 3. The temperature increases initially for a few ps due to the dynamic impact, which converts kinetic energy to thermal energy, but then drops rapidly via substrate cooling. Due to its higher thermal conductivity, the cooling rate in the Cu substrate case is about twice of the case of $\text{Cu}_{46}\text{Zr}_{54}$ glass substrate. The Cu nanocrystal formed on the Cu substrate has entropy lower than the SCGM by $\sim 1.5 \text{ J/mol/K}$ at 500 K.

We also examined nanodroplets of various sizes (4 to 30 nm in diameter; 2580 to 1 083 171 atoms) and larger substrates (up to 7 680 000 atoms), with a range of impact velocities (0.01–0.5 km/s), and various orientations for the Cu substrates [(100), (110), and (111)] and always obtain similar results. Our simulations show that nanodroplets $\leq 30 \text{ nm}$ in

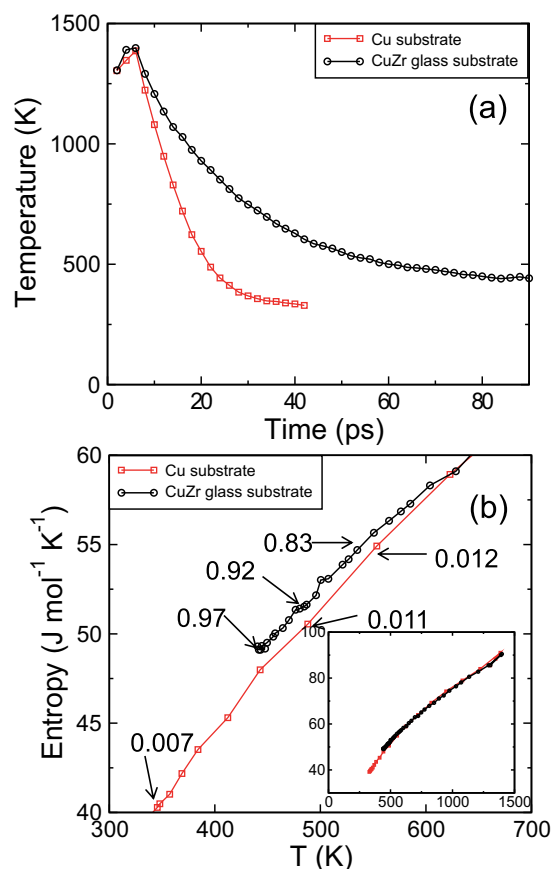


FIG. 3. (Color online) Temperature and entropy evolution of the 4-nm nano-droplets impacting at 0.5 km/s on crystalline or amorphous substrates. (a) For both substrates, the temperature increases for up to 6 ps after the initial impact and then decreases, with an exponential cooling rate (exponential fitting parameter) of $9.7 \times 10^{10} \text{ s}^{-1}$ for Cu substrate and $4.5 \times 10^{10} \text{ s}^{-1}$ for the glass substrate. (b) The entropy as a function of the temperature (below 700 K). The big difference between the crystal and amorphous substrates shows up below 700 K where the entropy of SCMG formed on amorphous substrate is about $0.2R$ higher than that of the nanocrystal formed on the Cu substrate at 500 K. Here, R is the gas constant. Inset shows the whole temperature range. The numbers shown are the ratio of HA index 2331 to the sum over all the cases for the first nearest neighbors.

diameter form SCMGs via ND-AS. We also performed the same simulations with another Cu-Zr potential,¹⁹ leading to nearly identical results.

For an impact velocity of 0.01 km/s, a nanodroplet at 1300 K and diameter of 30 nm achieves a cooling rate of $\sim 2 \times 10^{12} \text{ K/s}$, which we find is sufficient for SCMG formation on a glass surface. For an impact velocity of 0.5 km/s, a nanodroplet at 1300 K and diameter of 4 nm, achieves a cooling rate of $\sim 1 \times 10^{13} \text{ K/s}$, which we find is also sufficient for SCMG formation. However, for a crystalline substrate, we find that these same conditions lead to crystallization. Our interpretation is that the glass substrates lack the heterogeneous crystallization nucleation sites. That is, the high energy-barrier for homogeneous crystal nucleation leads to kinetics too slow to compete with glass transition, and thus to SCMG formation. The high temperature gradient near the substrate surface initiates the growth of the SCMG.

It has also been suggested that free-standing submicron droplets of high purity metals may become amorphous solid-like phases in vacuum via thermal radiation cooling.²⁰

We claim that two conditions, rapid quenching due to the size of the nanodrop hitting the cool substrate and the amorphous nature of the substrate, are both essential to obtain a single component amorphous metal. Evidence in favor of this is presented in Fig. 3(a), where the cooling for the Cu substrate is even more rapid than that for the amorphous substrate, but we find rapid crystallization of the droplet on the crystal substrate but not on the amorphous substrate. In addition, we did a simulation of annealing the amorphous droplet (4 nm in diameter) without substrates from 600 K to 300 K over 100 ps and found that the droplet retains the amorphous structure.

Of course, numerous droplets must be deposited to produce a macroscopic amorphous film. Thus, one must wonder whether the growth of the pure Cu amorphous film might eventually lead to nucleation of the crystal phase. To demonstrate that this does not occur we continued to impact nanodroplets (4 nm in diameter) of Cu at 1300 K onto the growing film until 180 nanodroplets had been added. We modeled this by constructing a $20 \times 3 \times 3$ array along the x, y, z directions, respectively (x is the impact direction), of nanodroplets (each 4 nm in diameter) spaced by $12 \text{ nm} \times 5 \text{ nm} \times 5 \text{ nm}$ using an impact velocity of 0.2 km/s (so that the time between successive nanodrops hitting the amorphous surface is larger than 40 ps during which the previous liquid droplets became solid amorphous). We find that the bulk film (now 18.5 nm thick) remains amorphous until the system reaches equilibrium. The combination of rapid cooling rate and amorphous substrates still avoids heterogenous nucleation of crystals. The high viscosities (low diffusion coefficient) of the SCMGs make the phase transition from amorphous to crystal phase kinetically unfavorable.

We have demonstrated that the synthesis of SCMGs via thermal spray of nanodroplets on amorphous substrates is viable for pure Cu, and we expect it to apply equally to other elemental metals. The thermal spray conditions required to form SCMGs are technically viable, and hence, we expect that ND-AS may provide opportunities for broad applications that fully exploit the uniqueness of metallic glasses.

This work was supported by the Department of Energy National Nuclear Security Administration PSAAP project at Caltech (DE-FC52-08NA28613) and the ASC/LDRD programs at LANL.

¹A. L. Greer, *Science* **267**, 1947 (1995).

²W. L. Johnson, *MRS Bull.* **24**, 42 (1999).

³A. Inoue, *Acta Mater.* **48**, 279 (2000).

⁴W. Klement, R. H. Willens, and P. Duwez, *Nature (London)* **187**, 869 (1960).

⁵Z. P. Lu, C. T. Liu, J. R. Thompson, and W. D. Porter, *Phys. Rev. Lett.* **93**, 245503 (2004).

⁶D. H. Xu, G. Duan, and W. L. Johnson, *Phys. Rev. Lett.* **93**, 245504 (2004).

⁷V. Ponnambalam, S. J. Poon, and G. J. Shiflet, *J. Mater. Res.* **19**, 1320 (2004).

⁸W. H. Wang, C. Dong, and C. H. Shek, *Mater. Sci. Eng. R.* **44**, 45 (2004).

⁹M. I. Mendeleev, M. J. Kramer, R. T. Ott, D. J. Sordet, D. Yagodin, and P. Popel, *Phil. Mag.* **89**, 967 (2009).

¹⁰S. Plimpton, *J. Comp. Phys.* **117**, 1 (1995).

¹¹J. D. Honeycutt and H. C. Andersen, *J. Phys. Chem.* **91**, 4950 (1987).

¹²Y. Qi, T. Cagin, W. L. Johnson, and W. A. Goddard III, *J. Chem. Phys.* **115**, 385 (2001).

¹³H. J. Lee, T. Cagin, W. L. Johnson, and W. A. Goddard III, *J. Chem. Phys.* **119**, 9858 (2003).

- ¹⁴G. Duan, D. Xu, Q. Zhang, G. Zhang, T. Cagin, W. L. Johnson, and W. A. Goddard III, *Phys. Rev. B* **71**, 224208 (2005).
- ¹⁵S. T. Lin, M. Blanco, and W. A. Goddard III, *J. Chem. Phys.* **119**, 11792 (2003).
- ¹⁶G. Y. Zhang, Q. An, and W. A. Goddard III, *J. Phys. Chem. C* **115**, 2320 (2011).
- ¹⁷T. A. Pascal, S. T. Lin, and W. A. Goddard III, *Phys. Chem. Chem. Phys.* **13**, 169 (2011).
- ¹⁸Y. Y. Li, S. T. Lin, and W. A. Goddard III, *J. Am. Chem. Soc.* **126**, 1872 (2004).
- ¹⁹Y. Q. Cheng, E. Ma, and H. W. Sheng, *Phys. Rev. Lett.* **102**, 245501 (2009).
- ²⁰Y. Kim, H. M. Lin, and T. F. Kelly, *Acta Metall.* **37**, 247 (1989).